IOSR Journal of Applied Chemistry (IOSR-JAC)
e-ISSN: 2278-5736.Volume 10, Issue 7 Ver. I (July. 2017), PP 35-43
www.iosrjournals.org

A Facile Plant Mediated Synthesis of Magnetite Nanoparticles Using Aqueous Leaf Extract of *Ficus hispida* L. for Adsorption of Organic Dye

A.V.Ramesh[1], B.Lavakusa[1], B. Satish Mohan[1], Y. Pavan Kumar[1], D.RamaDevi[2], K.Basavaiah[1]
[1]*Department Of Inorganic & Analytical Chemistry, Andhra University Visakhapatnam-530003, India.*
[2]*A.U. College Of Pharmaceutical Sciences, Andhra University, Visakhapatnam-530003, India.*

Abstract: *A facile and eco-friendly method for the synthesis of magnetite nanoparticles (Fe_3O_4 NPs) via Co-Precipitation in the presence of aqueous leaf extract of Ficus hispida L. The optical, crystalline, structural morphology and magnetic behaviour of the synthesized Fe_3O_4 NPs were characterized by Ultraviolet-Visible (UV-Vis), Fourier transform infrared (FTIR) spectroscopy, powder X-ray diffraction (XRD), field emission scanning electron microscopy (FESEM), and transmission electron microscopy (TEM) and vibrating sample magnetometer (VSM). The absorption spectrum reveals the peak at 379 nm, which confirm the formations of Fe_3O_4 NPs. XRD results reveals the formation of phase pure Fe_3O_4 NPs with cubic inverse spinel structure with crystallite sizes of 11.04 nm. The FESEM and TEM images clearly show that the spherical shape of Fe_3O_4 NPs with average particles size of 10.96 nm. Bright circular rings in the selected area electron diffraction (SAED) pattern showed good crystallinity. VSM results show super paramagnetic behaviour of Fe_3O_4 NPs. The synthesized Fe_3O_4 NPs have potential to adsorption of Methylene Blue(MB)*

Keywords*: Magnetite nanoparticles, Green Synthesis, Ficus hispida L. leaf, Methylene Blue dye.*

I. Introduction

During the past two decades metal oxide nanomaterials have attracted a great attention due to their unique optical, electrical, magnetic and electronic properties[1].Especially, the magnetic metal oxide nanoparticles received much attention for a wide range of applications such as catalysis, biosensors, ferrofluids, high density magnetic storage media, separation and purification of biomolecules[2-6]. Among all magnetic metal oxides, magnetite (Fe_3O_4) have emerged potential candidates for advance technological applications due to their low toxicity, biocompatibility and super paramagnetic behaviour [7-9]. Upto now, various morphologies, such as nanorods, nanowires, nanofibers, nanoflowers, nanotubes, nano cage, and nanoparticles have been prepared for Fe_3O_4 NPs by several chemical and physical approaches such as Co-Precipitation, hydrothermal, thermal decomposition of iron carbonyls, poloyl, electrochemical deposition, spray and laser pyrolysis and sono chemical method [10-20]. In all these methods, synthesis of Fe_3O_4 NPs uses toxic or potentially hazardious materials and requires more energy. Moreover, Fe_3O_4 NPs can easily aggregated below their critical particle size and limits their applications. Numerous approaches have been reported for the preparation of aggregate free Fe_3O_4 NPs by the use of surface capping agents such as polymers, long chain organic capping agents. However, these capping agents have a potential toxicity to the environment and public health. Therefore, it is highly desirable to develop simple bio-compatible and green methods for synthesis of Fe_3O_4 NPs. More recently, use of biomaterials such as microbial, fungi and plant extracts for the preparation of variety of metal oxide nanoparticles due to their nontoxic nature and eco-friendly. The plant extract assisted synthesis of Fe_3O_4 NPs has been quite limited and few plant extracts mediated works have been reported. For example, *Tridax procumbens* , *Artemisia annua* , leaf extract of *Perilla frutescens* and *caricaya papaya* and also seed extract of *grape proanthocyanidin* [21-25] .So far no reports were available for synthesis of Fe_3O_4 NPs using the aqueous leaf extract of *Ficus hispida* L. In this work, for the first time, we have synthesized Fe_3O_4 NPs via plant mediated green synthesis approach using aqueous leaf extract of *Ficus hispida* L. The synthesis carried out in an aqueous medium, aqueous leaf extract of *Ficus hispida* L. act as reducing and capping agent for Fe_3O_4 NPs. As prepared Fe_3O_4 NPs using aqueous leaf extract of *Ficus hispida* L were characterized by range of spectroscopic and microscopic techniques such as UV-Visible(UV-Vis), Fourier transform infrared (FTIR) spectroscopy, powder X-ray diffraction (XRD), Field emission scanning electron microscopy (FESEM), and Transmission electron microscopy (TEM) and Vibrating sample magnetometer (VSM).

II. Experimental

2.1 Materials

Analytical grade Iron (II) sulfate hepta hydrate ($FeSO_4.7H_2O$), Iron (III) chloride hexa hydrate ($FeCl_3.6H_2O$),NH_3,Methylene blue were purchased from Merck, India and used without further purification. The leaves of *Ficus hispida* L. were collected from forest of Chintapalli, Andhra Pradesh, India. Milli-Q water was used throughout the synthesis process.

2.2 Preparation of plant extract

The fresh leaves of *Ficus hispida* L. washed thoroughly with running tap water and followed by Milli-Q water to remove the dust, adhering soil and the leaves were dried under shade for 15 days and make powdered using blender. The extract was prepared by dissolving 5 grams of leaf powder in 100 ml of Milli-Q water and boiled at 60 ^{0}C for 20 min. Then the aqueous leaf extract was filtered through the Whatman NO.1 filter paper to separate out the broth and the filtrate was stored at 4 ^{0}C for the preparation of Fe_3O_4 NPs.

2.3 Synthesis of Fe_3O_4 NPs

Fe_3O_4 NPs were synthesized based on co-precipitation method in the presence of aqueous leaf extract of *Ficus hispida* L. as a capping agent. In a typical synthesis, 2:1 molar ratio of $FeCl_3.6H_2O$ (0.11 g) and $FeSO_4.7H_2O$ (0.556 g) were dissolved in a 85 mL Milli-Q water under ultrasonication in a 250 mL Erlenmeyer flask at room temperature. Then the reaction was allowed for 60 minutes to proceeded at 80^{0}Cwith constant stirring under nitrogen atmosphere .Then, 10 mL of 5 % aqueous leaf extract of *Ficus hispida* L. was quickly added in to the above reaction mixture and 5 mL of 25% NH_3 was added drop wise to the reaction mixture to adjust the pH = 10.The formation of Fe_3O_4NPs was marked by the appearance of a black precipitate, and the Fe_3O_4NPs were separated by centrifuging at 5000 rpm. The product was washed periodically with Milli-Q water and ethanol and then dried in the vacuum at room temperature.

2.4 Characterization

The absorption spectra of as prepared Fe_3O_4NPs were recorded using a Shimadzu (2450 – SHIMADZU) spectrometer. Fourier transform-infrared (FTIR) spectra were recorded in the range of 4000-400 cm^{-1} with a SHIMADZU-IR PRESTIGE-2 Spectrometer. Powder samples were mixed thoroughly with potassium bromide (KBr) and pressed into thin pellets. The powder X-ray diffraction (XRD) patterns were obtained by PANalytical X'pert pro diffractometer at 0.02 degree/sec scan rate with Cu-kα_1 radiation (1.5406 A^0, 45 kV, 40 mA).Morphology of Fe_3O_4NPs was investigated by using FESEM (FESEM, Zeiss Ultra-60) equipped with X-ray energy dispersive spectroscopy (EDS). TEM images were obtained (TEM model FEI Technai 20 U Twin) at an accelerating voltage of 120 and 200 kV.The room temperature magnetization of Fe_3O_4NPswas measured using vibrating sample magnetometer (VSM Lakeshore 665, USA).

2.5 Batch mode adsorption studies

Batch adsorption efficiency of synthesized Fe_3O_4 NPs experiments was carried out at room temperature (300 K) using Methylene Blue as a model water pollutant. Typically, 50 mg of Fe_3O_4NPs was mixed with 50 mL of known concentration of dye solution. The solution pH was adjusted by HCl (0.1 M) or NaOH (0.1 M). The flasks were stirred for the specified time period and sample from each flask was withdrawn at the desired time of reaction. The synthesized Fe_3O_4NPs were recovered by an external magnet. The residual dye concentration was determined by UV-Visible spectrophotometer by measuring the absorbance at a wavelength of maximum (λ_{max}= 664 nm) absorbance of MB. The amount of adsorbed MB (q) onto synthesized Fe_3O_4 NPs was expressed in mg of dye per gram of Fe_3O_4NPs, as shown in the Eq. (1):

$$q = (C_0 - C)*V/m \qquad \text{----------} \qquad (1)$$

Where q is adsorption capacity of MB in ($mg.g^{-1}$) at time t, C_0 represents the initial MB concentration in $mg.L^{-1}$, C is the concentration of MB in mg/L after adsorption at a time't', V is the volume of MB solution in L, and m is the mass of synthesized Fe_3O_4 NPs in grams. The adsorption phenomenon was evaluated by adsorption isotherms and kinetic models

III. Result And Discussion

Fe_3O_4 NPs were prepared via co-precipitation method by adding a base (25% NH_3) to an aqueous mixture of Fe^{3+} and Fe^{2+} salts at a 2:1 molar ratio in presence of the aqueous leaf extract of *Ficus hispida* L. The phytochemicals present in the aqueous leaf extract of *Ficus hispida* L. are responsible for the formation of Fe_3O_4 NPs. After addition of 25% NH_3 and stirring the reaction mixture for 1 h, the colour of the reaction mixture of Fe^{2+} and Fe^{+3} salts and aqueous leaf extract of *Ficus hispida* L. turned from light rose red to black, which indicates the formation of Fe_3O_4 NPs. The UV-Vis absorption spectra of synthesized Fe_3O_4 NPs and aqueous

leaf extract of *Ficus hispida* L. were depicted in Fig 2. The aqueous leaf extract of *Ficus hispida* L. has a strong absorption bands at 235 and 265 nm which are attributed to the presence of terpenoids, alkaloids, phenolic acid, flavoniod, tannins and carbohydrates in aqueous extract. The characteristic absorption band at 379 nm indicates the formation of Fe_3O_4 NPs which is primarily due to the absorption and scattering of light by Fe_3O_4 NPs. Moreover, the absence of the leaf extract peak of *Ficus hispida* L. at 235 and 265 nm in the Fe_3O_4 NPs spectrum clearly indicates terpenoids, alkaloids, phenolic acid, flavoniod, tannins and carbohydrates phytochemicals act as reducing and capping agent for synthesis of Fe_3O_4 NPs.

Fig. 1 Images of of *Ficus hispida* L plant

The plant *Ficus hispida* L. belongs to the Moraceae family and its leaves used as an indigenous traditional medicine [26]. The extracts of all parts of the plant have been reported to be antidysenteric and to have activity against jaundice, hypoglycemic activity,antidiabetic activity and hemorrhage [27-29]. Leaf extract of *Ficus hispida* L. contains alkaloids, carbohydrates, proteins, amino acids, sterols, phenols, flavonoids, glycosides, saponins, and terpenes. Phytochemicals present in leaf extract of *Ficus Hispida* L. can used as reducing and capping agent for the formation of magnetite nanoparticles.

3.1 UV-Vis, XRD Characterization of as prepared Fe_3O_4 NPs

The UV-Vis absorption spectra of both aqueous leaf extract of *Ficus hispida* L. and synthesized Fe_3O_4 NPs were depicted in Fig 2. The characteristic absorption peak observed at 379 nm which indicates the formation of Fe_3O_4 NPs. As the concentration of bark extract increases, the absorption intensity of synthesized Fe_3O_4 NPs also increases.

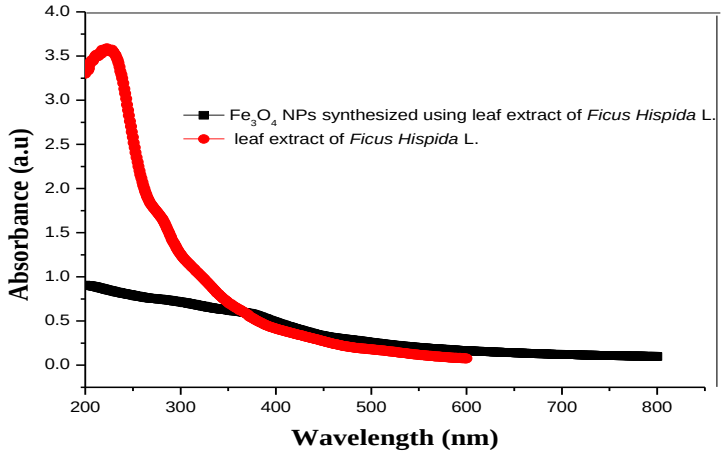

Fig .2 The UV–vis spectra of 5 % aqueous leaf extract of *Ficus hispida* L. and Fe_3O_4 NPs synthesized using 5% aqueous leaf extract of *Ficus hispida* L. **.** at 350 K, and P^H= 10 respectively.

The crystalline nature of Fe_3O_4 NPs was confirmed using powder XRD. The XRD pattern of Fe_3O_4 NPs synthesized using aqueous leaf extract of *Ficus hispida* L. was shown in Fig 3. The Bragg reflection peaks were observed at 2θ values of 30.19, 35.736, 43.40,53.8, 57.37,62.93,74.7 which could be indexed to

(220),(311), (400), (422),(511), (440) and (533) planes of inverse cubic spinel phase of pure Fe_3O_4 NPs (JCPDS 19-0629). The intense reflection at (311) plane in contrast to the other of planes may specify the growth direction of the nanocrystals.

The average crystallite sizes of the Fe_3O_4NPs were estimated by the Scherrer equation

$$D = k\lambda / \beta\cos\theta \qquad \text{(Eq.1)}$$

Where D is particle diameter size, K is a constant equals 1, λ is wavelength of X-ray source (0.1541 nm), β is the full width at half maxima (FWHM) and θ is the diffraction angle corresponding to the lattice plane The average crystallite size of Fe_3O_4 NPs according to Scherrer equation with the width of (311) plane is found to be11.04 nm.

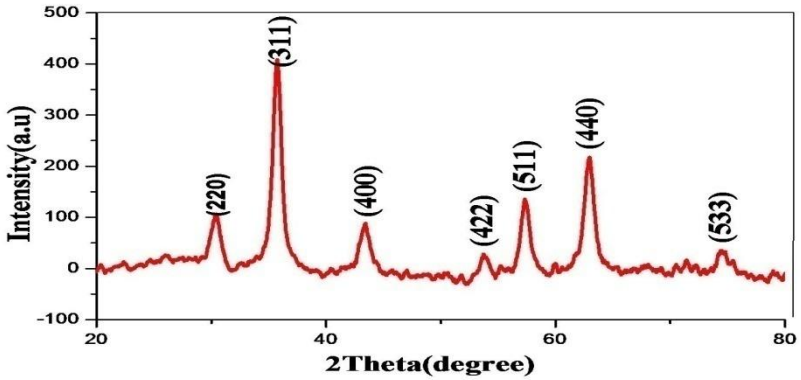

Fig. 3 Powder XRD patterns of Fe_3O_4 NPs synthesised using aqueous leaf extract of *Ficus hispida* L.

3.2Morphology

Surface morphology as synthesised Fe_3O_4NPs was investigated by FESEM and TEM. Representative FESEM images of Fe_3O_4NPs depicts in Fig.4 (a-c). FESEM images of Fe_3O_4 NPs show spherical shape. Fig 5(d) show the EDS spectrum of Fe_3O_4 NPs and it shows that the presence of Fe and O atoms with 63.75%, 29.37% weight value respectively. EDS spectrum also reveals that the presence of C (6.87) % are the source of leaf extract of *Ficus hispida* L.

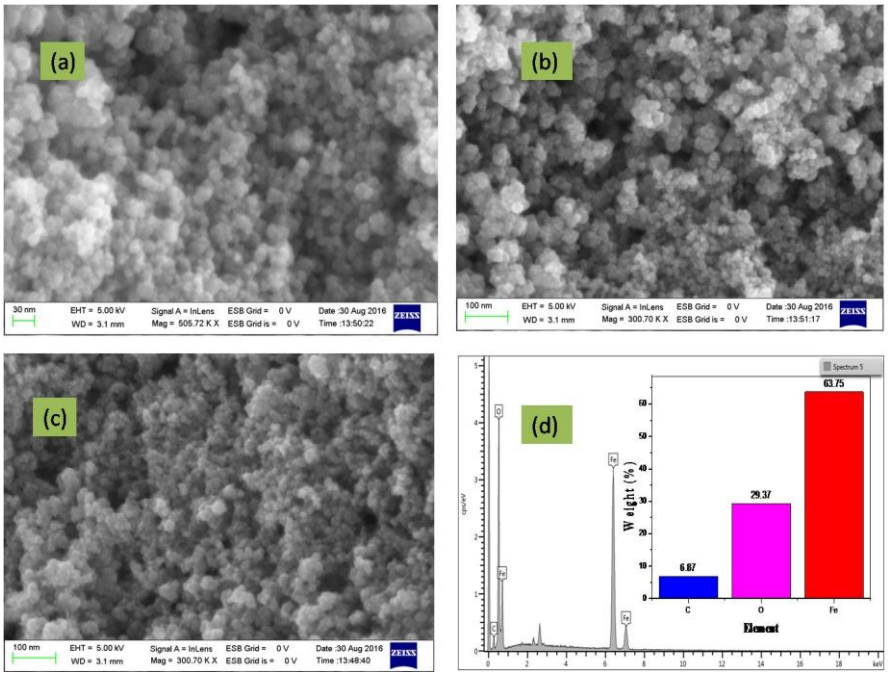

Fig.4 (a, b and c) FESEM images and (d) Energy dispersive X-ray spectroscopy (EDS) of Fe_3O_4 NPs synthesized using aqueous leaf extract of *Ficus hispida* L.

TEM images of Fe_3O_4NPs synthesized using aqueous leaf extract of *Ficus hispida* L**.** represent in Fig 5(a-b). As can be seen in Fig 5(a-b), the morphology of the Fe_3O_4 NPs was found to be cubic morphology with an average particle size 10.96 nm. It is very close to crystallite size (11.04). The selected area electron diffraction (SAED) pattern of the Fe_3O_4 NPs shows in Fig 5 (c). The ring-like diffraction pattern indicates that the as synthesizedFe_3O_4 NPs are crystalline. The size distribution histogram of synthesized Fe_3O_4 NPs shows in Fig 5 (d).

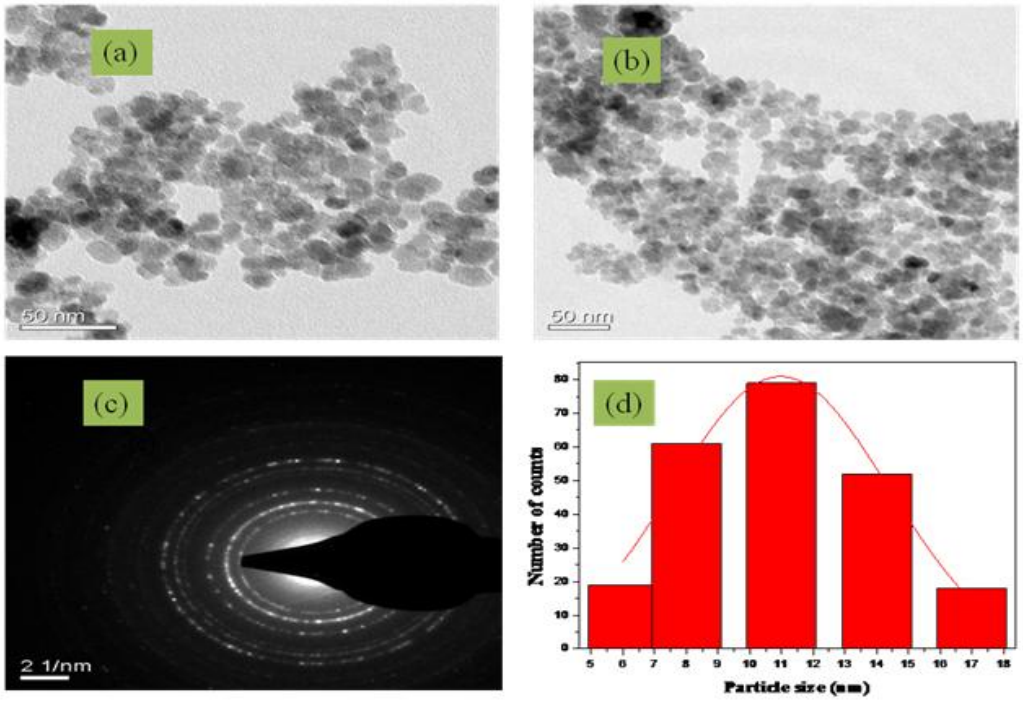

Fig 5 (a and b) Representative TEM images and (c) Selected Area Electron Diffraction (SAED) and(d) size distribution histogram of Fe_3O_4 NPs synthesized using aqueous leaf extract of *Ficus hispida* L.

3.3Magnetic property

The magnetic property of synthesized Fe_3O_4 NPs was measured at room temperature by a Vibrating sample magnetometer (VSM). The magnetization curve of the synthesized Fe_3O_4 NPs is presented in Fig.6. The sigmoidal shape of VSM curve of the synthesized Fe_3O_4 NPs without hysteresis loop demonstration of super paramagnetic behaviour with the saturation magnetization (Ms) value 100 emu/g at room temperature.

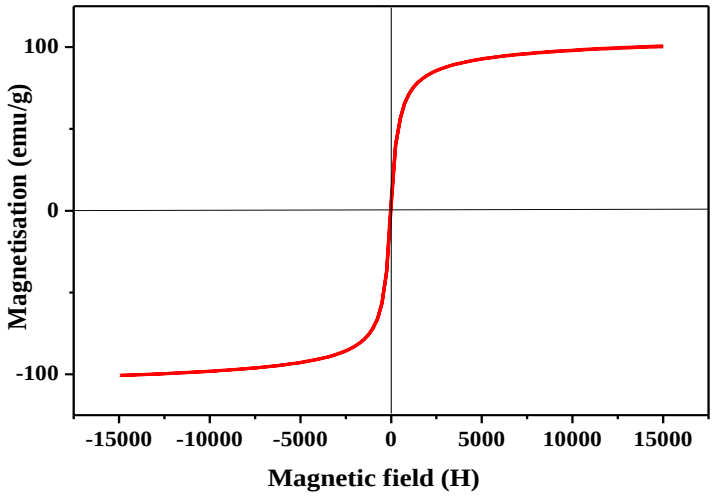

Fig. 6 The room temperature magnetization curve of Fe_3O_4 NPs synthesized using aqueous leaf extract of *Ficus hispida* L.

3.4 FTIR characterisation of as prepared Fe_3O_4 NPs

FTIR spectra were recorded to identify the functionalities found on aqueous leaf extract of *Ficus hispida* L. and Fe_3O_4 NPs. As shown in Fig 7(a-b), both FTIR spectra of and Fe_3O_4 NPs obtained from aqueous leaf extract of *Ficus hispida* L. and aqueous leaf extract of *Ficus hispida* L. extract have close similarities, with some marginal shifts in peak position, clearly indicate the presence of phtoconstituents in the leaf extract act as a reducing and capping agent to the Fe_3O_4 NPs. The phytochemical analysis of aqueous leaf extract of *Ficus hispida* L. based on FTIR spectrum strongly suggested the presence of flavoniods, tannins, carbohydrates and polyphenols, apart from other phytochemicals, which were mainly responsible for the preparation of the Fe_3O_4NPs. The FTIR spectrum of the aqueous leaf extract of *Ficus hispida* L. exhibited characteristic stretching frequencies at 3423,2926,2360,1622,1436,1315,1054,889,781,668cm^{-1}.

The characteristic band at 3423, 2926, 1622 $cm^{-1}$are ascribed to the presence of O-H group of the phenolic compound, C-H group of alkane, C=C group of terpenoids respectively. In the case of synthesized Fe_3O_4 NPs, a there was a shift in the absorbance peak of O-H group from 3423 to 3402 cm^{-} indicates O-H group of the phenolic group involved in the capping of Fe_3O_4NPs. There was also shift in the absorbance peak of C=C group of terpenoids from 1622 to 1628 cm^{-1}.Also, a characteristic additional peak formed at 584 $cm^{-1}$was observed for in the case of Fe_3O_4 NPs which are due to characteristic stretching vibration of Fe-O. Hence, FTIR analyses were suggested that the effective capping of *Ficus hispida* L. leaf extract to synthesized Fe_3O_4NPs .

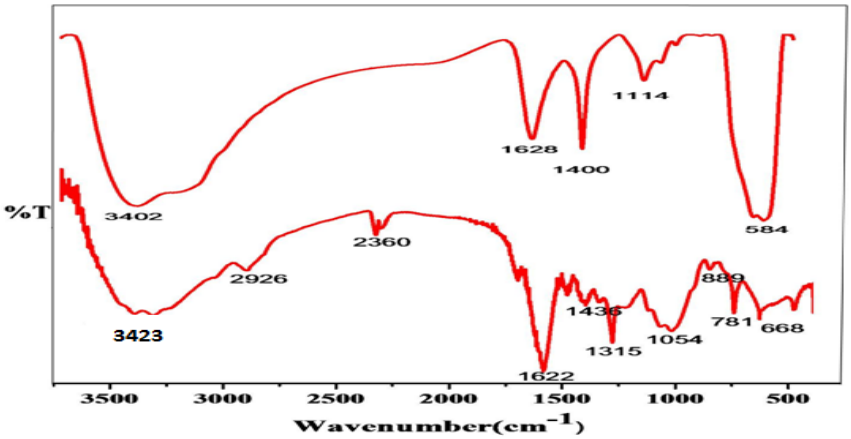

Fig. 7 FTIR spectra of (a) Fe_3O_4 NPs synthesised using aqueous leaf extract of *Ficus hispida* L. and (b) aqueous leaf extract of *Ficus hispida* L.

IV. Adsorption Studies

The time-dependent UV–vis absorption spectra of MB in the solution at time 't' after the adsorption by synthesized Fe_3O_4 NPs is shown in Fig. 8. The adsorption after 180 min there was not observed a further reduction of MB peak at 664 nm which ascribed to adsorption equilibrium was attained at the end of 180 min. Fig. 9 (a-b) is depicted that at the adsorption equilibrium (180 min), adsorption of Fe_3O_4NPs for MB [at 300 K, pH = 11], were found to be 91 %, 89%, 80% for concentration of 5 mgL^{-1}, 10 mgL^{1}, 15 mgL^{-1}MB respectively.

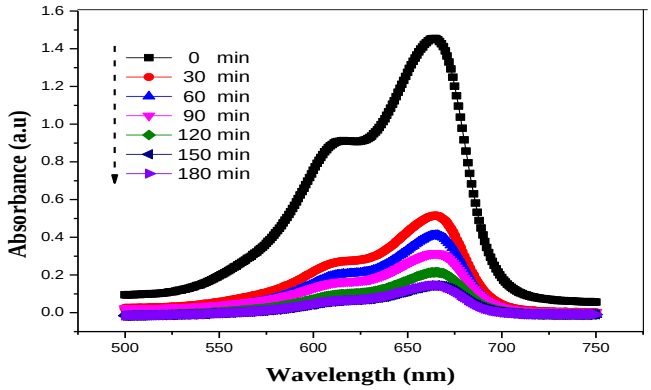

Fig.8 The UV–Vis absorption spectra of MB (10 mgL^{-1}) adsorbed by synthesized Fe_3O_4 NPs at different time

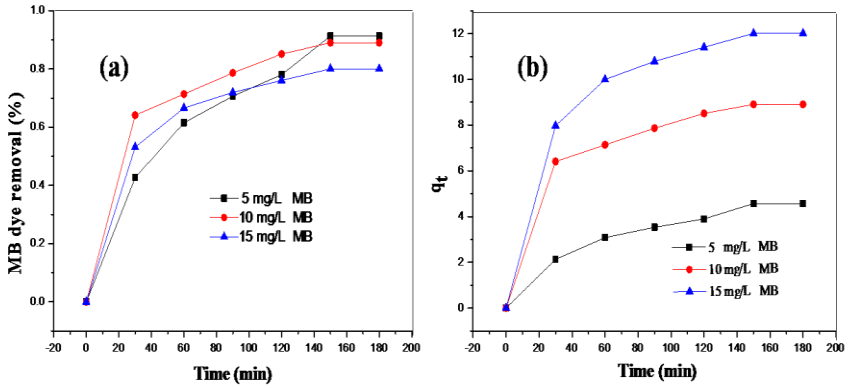

Fig.9 (a) The percentage (%) of dye adsorption removal, and (b) the amount of MB dye adsorbed (q in $mg.L^{-1}$) at various concentration of MB onto Fe_3O_4 NPs.

4.1 Adsorption kinetics

The adsorption kinetics of MB on synthesized Fe_3O_4 NPs was conducted at a different concentration of MB. Fig. 9(a-b) shows that the adsorption rate of MB on to synthesized Fe_3O_4 NPs at a different initial concentration of 5 mgL^{-1}, 10 mgL^{-1}, 15 $mgL^{-1}$of MB (at pH = 11 and 300 K). As shown in Fig. 9(b), the adsorption process was fast for the first 30 minuets and gradually reached to equilibrium at the end of180 min. The kinetics of adsorption of MB on synthesized Fe_3O_4 NPs was investigated by pseudo-first-order [30] Eq. (3) and the pseudo-second-order Eq. (4) kinetic models. The pseudo-first-order kinetic model is described by the equation:

$$\log (q_e - q_t) = \log q_e - (k_1/2.303) * t \qquad \text{Eq.(3)}$$

Where k_1 (min^{-1}) is the pseudo-first-order rate constant of adsorption, qt (mg/g) and q_e (mg/g) are the amounts of the MB adsorbed at time t and at equilibrium. k_1 (min^{-1}) was determined from the slope of the plot of log (qe-qt) vs t (Fig. 10(a)) and it was obtained that the correlation coefficient value (R^2) is 0.925.
Moreover, to validate the kinetic of adsorption of MB pseudo-second-order kinetic model was also investigated.

$$t/q_t = 1/k_2\, q_e^{\,2} + (1/q_e) * t \qquad \text{Eq (4)}$$

Where k_2 (g/mg min^{-1}) is the pseudo-second-order rate constant, q_t (mg/g) and q_e (mg/g) are the amount of the MB adsorbed at time t and at equilibrium. The values of q_e and $k_2$can be calculated from the slope and intercept of a plot of t/q_t vs t (Fig. 10 (b)). For this plot, correlation coefficient value (R^2) was found to be 0.98897
.It is concluded that the adsorption of MB on synthesized Fe_3O_4NPs was found to be a pseudo-second-order kinetic model and this implies that the adsorption process more likely proceeds through electrostatic interaction of MB and surface of synthesized Fe_3O_4 NPs, also called by chemisorption process[31].

4.2 Adsorption isotherm

Adsorption isotherm analyses are employed to investigate the maximum adsorption capacity of synthesized Fe_3O_4 NPs. The equilibrium adsorption isotherm parameters of MB on synthesized Fe_3O_4 NPs were analyzed using Langmuir and Freundlich isotherm models [32-33]. The Langmuir equation can be expressed as (Eq.5):

$$C_e/q_e = C_e/Q_0 + 1/\, Q_0 b_L \qquad \text{Eq(5)}$$

Where q_e(mg/g) is the equilibrium adsorption capacity of MB on the adsorbent, C_e(mg/L) is the equilibrium concentration of MB in the solution, Q_0 (mg/g) is the maximum capacity of adsorbent, and b (L/mg) is the equilibrium constant relating to the enthalpy of process. Fig.10(c) shows that the experimental data well fitted to the Langmuir adsorption isotherm and it was found to be 16.39344mg/g maximum adsorption capacity. The correlation coefficient (R^2) and equilibrium constant (b_L) values were found to be 0.9875 and 0.98387respectively. Besides, dimensionless factor (R_L) of the Langmuir adsorption isotherm parameter calculates using Eq. 5. The R_L value was obtained 0.179618 which is in between 0 and 1. This indicates that the adsorption of MB on Fe_3O_4 NPs is thermodynamically favorable.

$$R_L = 1/(1+b_L * C_0) \qquad (\text{Eq. 6})$$

Where C_0 (mg/g) is initial MB concentration, b_L (L/mg) is the Langmuir constant. For unfavourable sorption, RL > 1; for favourable sorption, $0< R_L< 1$; for irreversible sorption RL < 0; for linear sorption, $R_L< 1$
The Freundlich isotherm (Eq. 7) can be expressed as:

$$\log q_e = \log k_f + 1/n \log C_e \qquad \text{(Eq.7)}$$

q_e(mg/g), is the equilibrium adsorption capacity of MB on the synthesized Fe_3O_4 NPs, k_f(mg/g), 1/n are Freundlich constants representing the adsorption capacity (adsorption coefficient) at unit equilibrium concentration, and adsorption intensity. The value of Freundlich constant 'n' is 2.01.For this adsorption, n>1 indicating that MB favorably adsorbed on synthesized Fe_3O_4 NPs. The correlation coefficient values of Langmuir model (R^2=0.9875) more close to unity than Freundlich model (R^2=0.8883), which indicates that the experimental data best fit with the Langmuir isotherm. The monolayer adsorption maximum adsorption capacity (Q_0) of synthesized Fe_3O_4 NPs was found to be 16.39344 mg/g. This figure indicates that the *Ficus hispida* L. assisted synthesized Fe_3O_4 NPs has comparative adsorption efficiency towards organic dyes.

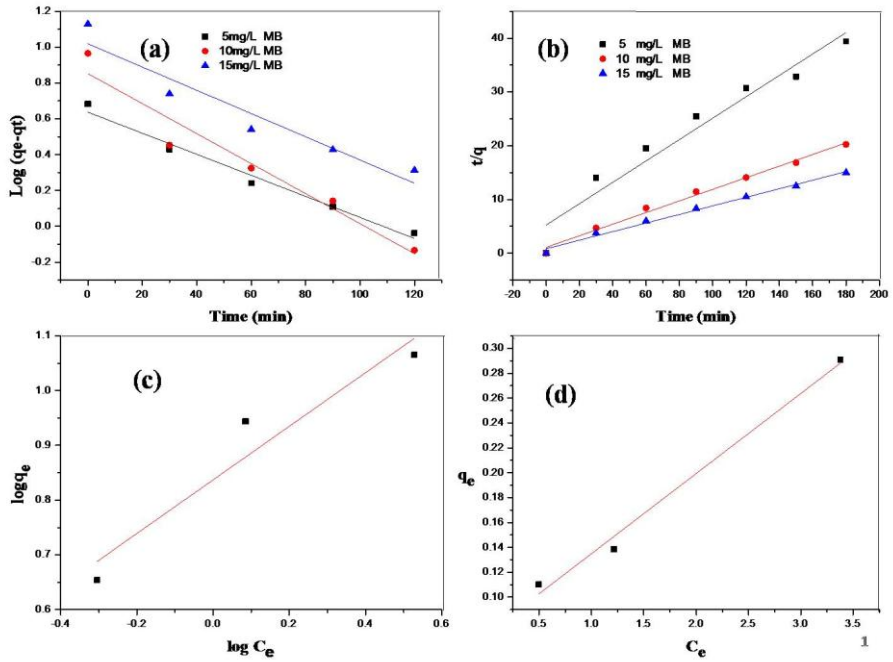

Fig.10 (a) Pseudo-first-order, (b) Pseudo-first-order kinetics plots, (c) Freundlich and (d) Langmuir adsorption isotherm plots of MB adsorption to synthesised Fe_3O_4 NPs.

Table 1: The kinetic parameters calculated from Pseudo-first and Pseudo second order kinetics model on adsorption of MB onto the synthesized Fe_3O_4 NPs

Parameters	**Initial concentration of dye**		
	5 ppm	10 ppm	15 ppm
q_e,exp. (mg.g)	4.56643	8.9021	12.00699
	Pseudo first order kinetics		
k_1 (min $^{-1}$)	0.013519	0.019276	0.014923
$q_e$cal (mg/g)	4.336207	7.12164	10.43999
R^2	0.97506	0.925	0.89399
	Pseudo second order kinetics		
k_2 (g/mg/min)	0.03787	0.09808	0.094543
$q_e$cal (mg/g)	5.027652	9.263548	12.54705
R^2	0.93528	0.98897	0.9897

Table 2: The Langmuir and Freundlich adsorption Isotherm parameters for adsorption of MB on synthesized Fe_3O_4 NPs

Isotherm models	**Parameters**		
Langmuir Isotherm	Q_0 (mg/g)	b_L(L/mg)	R^2
	16.39344	**0.98387**	**0.9875**
Freundlich Isotherm	**1/n**	**k_f (mg$^{1-1/n}$ L$^{1/n}$ g^{-1})**	**R^2**
	0.497	**7.413102**	**0.8883**

V. Conclusion

We have synthesized for the first time Fe_3O_4 NPs using aqueous leaves extract of *Ficus hispida* L. The synthesised Fe_3O_4 NPs have shown characteristic absorption band at 379 nm. XRD study of the synthesised Fe_3O_4 NPs has shown cubic inverse spinel structure with crystallite sizes of 11.04 nm. The FESEM and TEM images were clearly shown that the spherical shape of Fe_3O_4 NPs with average particles size of 10.96 nm. The

obtained magnetite nanoparticles exhibited super paramagnetic behaviour with the saturation magnetization (Ms) value 100 emu/g at room temperature. The synthesized Fe_3O_4 NPs have potential to adsorption of MB.

Acknowledgements

The author is grateful to UGC-SERO, Hyderabad for awarding teacher fellowship under FDP, XII plan of UGC,

References

[1]. Miller, M.M.; Prinz, G.A.; Cheng, S.F.; Bounnak, S. Detection of a micron-sized magnetic sphere using a ring-shaped anisotropic magnetoresistance-based sensor: A model for a magnetoresistance-based biosensor. *Appl. Phys. Lett.* **2002**, *81*, 2211–2213.

[2]. Zhang, J.L.; Wang, Y.; Ji, H.; Wei, Y.G.; Wu, N.Z.; Zuo, B.J.; Wang, Q.L. Magnetic nanocomposite catalysts with high activity and selectivity for selective hydrogenation of *ortho*-chloronitrobenzene. *J. Catal.* **2005**, *229*, 114–118.

[3]. Jeyadevan, B.; Chinnasamy, C.N.; Shinoda, K.; Tohji, K.; Oka, H. Mn-Zn ferrite with higher magnetization for temperature sensitive magnetic fluid. *J. Appl. Phys.* **2003**, *93*, 8450–8452.

[4]. Sun, S.H.; Murray, C.B.; Weller, D.; Folks, L.; Moser, A. Monodisperse FePt nanoparticles and ferromagnetic FePt nanocrystal superlattices. *Science* **2000**, *287*, 1989–1992

[5]. Mahdavi, M.; Ahmad, M.B.; Haron, M.J.; Gharayebi, Y.; Shameli, K.; Nadi, B. Fabrication and characterization of SiO2/(3-aminopropyl) triethoxysilane-coated magnetite nanoparticles for lead (II) removal from aqueous solution. *J. Inorg. Organomet. Polym. Mater.* **2013**, *23*, 599–607.

[6]. JGuoa, J.; Wanga, R.; Tjiu, W.W.; Pan, J.; Liu, T. Synthesis of Fe nanoparticles@graphene composites for environmental applications. *J. Hazard. Mater.* **2012**, *225–226*, 63–73.

[7]. Guptaa, A.K.; Gupta, M. Synthesis and surface engineering of iron oxide nanoparticles for biomedical applications. *Biomaterials* **2005**, *26*, 3995–4021.

[8]. JGuoa, J.; Wanga, R.; Tjiu, W.W.; Pan, J.; Liu, T. Synthesis of Fe nanoparticles@graphene composites for environmental applications. *J. Hazard. Mater.* **2012**, *225–226*, 63–73.

[9]. U. Jeong, X.W. Teng, Y. Wang, H. Yang, Y.N. Xia, Advanced Materials 12 (1) (2007) 33-60.

[10] Y. Zhao, Z. Qiu, J. Huang, Chinese Journal of Chemical Engineering 16 (3) (2008) 451-455.

[11] B. Mao, Z. Kang, E. Wang, S. Lian, L. Gao, C. Tian, C. Wang, Materials Research Bulletin 41 (2006) 2226.

[12] K. Woo, J. Hong, J.P. Ahn, Journal of Magnetism and Magnetic Materials 293 (2005) 177.

[13] U.T. Lam, R. Mammucari, K. Suzuki, N.R. Foster, Industrial and Engineering Chemistry Research 47 (3) (2008) 599-614.

[14] R.P. Bagwe, J.R. Kanicky, B.J. Palla, P.K. Patanjali, D.O. Shah, Critical Reviews in Therapeutic Drug Carrier Systems 18 (1) (2001) 77-140.

[15] F. Fievet, J.P. Lagier, B. Blin, B. Beaudoin, M. Figlarz, Solid State Ionics 198 (1989) 32.

[16] H.R. Kahn, K. Petrikowski, Journal of Magnetism and Magnetic Materials 215-216 (2000) 526.

[17] C. Prcharroman, T. Gonzalez-Carreno, J.E. Iglesias, Physics and Chemistry of Minerals 22 (1995) 21.

[18] S. Veintemillas-Vendaguer, M.P. Morales, O. Bomati-Miguel, C. Batista, X. Zhao, P. Bonville, R.P. Alejo, J. Ruiz-Cabello, M. Santos, J. Tendillo-Cortijo, J. Ferreiros, Journal of Physics 37 (2004) 2054.

[19] V.F. Puntes, K.M. Krishnan, A.P. Alivisatos, Topics in Catalysis 19 (2002) 145.

[20] H.G. Rotstein, R. Tannenbaum, Journal of Physical Chemistry B 106 (2002) 146.

[21] Senthil M, Ramesh C (2012) Biogenic synthesis of Fe_3O_4 nanoparticles using *Tridax procumbens* leaf extract and its antibacterial activity on pseudomonas aeruginosa. Dig J Nanomater Biostruct 7(4):1655–1659

[22] Basavegowda N, Magar KBS, Mishra K, Lee YR (2014) Green fabrication of ferromagnetic Fe_3O_4 nanoparticles and their novel catalytic applications for the synthesis of biologically interesting benzoxazinone and benzthioxazinone derivatives. New J Chem 38(11):5415–5420

[23] Basavegowda N, Mishra K, Lee YR (2014) Sonochemically synthesized ferromagnetic Fe_3O_4 nanoparticles as a recyclable catalyst for the preparation of pyrrolo [3, 4-*c*] quinoline-1,3-dione derivatives. RSC Adv 4(106):61660–61666

[24] Latha N, Gowri M (2014) Biosynthesis and characterisation of Fe_3O_4 nanoparticles using *Caricaya papaya* leaves extract. Int J Sci Res 3(11):1551–1556

[25] Narayanan S, Sathy BN, Mony U, Koyakutty M, Nair SV, Menon D (2012) Biocompatible magnetite/gold nanohybrid contrast agents via green chemistry for MRI and CT bioimaging. ACS Appl Mater Interfaces 4(1):251–260

[26] Manandhar, N.P(1995) A Survey of medicinal plants of jajarkot district, Nepal. *J. Ethnopharmacol*., v.48, p.1-6.

[27] Nadkarni, K.M(, 1976)*Indian materia medica*. New Delhi: Narayana Publishersv.1, p.1031.

[28] Rastogi, R.; Mehrotra, B.N(1993)*Compendium indian medicinal plants*. New Delhi: CDRI, Lucknow, v.2, p.27. (Publication and Information Directorate).

[29] Sergio, R.; Peraza, S (2002) Constituents of leaves and twigs of *Ficus hispida*. *Plant Med.*, v.68, p.186-188.

[30]. S. Lagergren, *KungligaSvenskaVetenskapsakademiensHandlingar*, 1898, 24, 1-39.

[31]. Y. Ho and G. Mckay, *Process Biochemistry*, 1999, 34, 451–465.

[32]. I. Langmuir, *Journal of the American Chemical Society*, 1916, 38, 2221–2295.

[33]. H.M.F. Freundlich, *Journal of Physical Chemistry*, 1906, 57, 385–471.

IOSR Journal of Applied Chemistry (IOSR-JAC) is UGC approved Journal with Sl. No. 4031, Journal no. 44190.

A.V. Ramesh. "A Facile Plant Mediated Synthesis of Magnetite Nanoparticles Using Aqueous Leaf Extract of *Ficus Hispida* L. for Adsorption of Organic Dye." IOSR Journal of Applied Chemistry (IOSR-JAC) 10.7 (2017): 35-43.